Every Spectral Switch Costs Memory: Sharp Robust Wigner–Smith Speed Limits for Passive Quantum Networks

Lluis Eriksson

10 August 2026

Abstract

Exact interpolation can force the internal degree of a passive network, but laboratory calibrations are approximate. We prove a sharp frequency-domain speed limit that needs neither exact zeros nor analytic continuation away from the measured frequency axis. Let $S(\mathrm{e}^{\mathrm{i}\theta})$ be an absolutely continuous unitary scattering path with positive Wigner–Smith generator

$$Q(\theta) = -\mathrm{i}S(\mathrm{e}^{\mathrm{i}\theta})^* \partial_\theta S(\mathrm{e}^{\mathrm{i}\theta}) \succeq 0.$$

A fixed k-dimensional input subspace is routed approximately into one output sector at one end of a frequency arc and into its orthogonal complement at the other. If the two amplitude leakages are $\varepsilon_p, \varepsilon_s$ and

$$\alpha = \left[\frac{\pi}{2} - \arcsin \varepsilon_p - \arcsin \varepsilon_s\right]_+,$$

then every such transition obeys

$$\int_I \operatorname{tr} Q \, \mathrm{d}\theta \geq 2k\alpha, \qquad \int_I \lambda_{\max}(Q) \, \mathrm{d}\theta \geq 2\alpha.$$

Consequently a transition across width Δ forces peak trace delay at least $2k\alpha/\Delta$ and peak proper delay at least $2\alpha/\Delta$. For disjoint arcs the costs add. If S is rational inner of McMillan degree n, $\int_{\mathbb{T}} \operatorname{tr} Q = 2\pi n$; hence M alternating pass/stop pairs imply

$$\boxed{n \geq \frac{2Mk}{\pi} \left[\frac{\pi}{2} - \arcsin \varepsilon_p - \arcsin \varepsilon_s\right]_+.}$$

At zero error this is $n \geq Mk$. A $2k$-port interferometric family of degree Mk saturates the global law exactly and saturates both local laws for every admissible error pair, proving all constants optimal. The proof combines canonical-angle geometry on the Grassmannian with two sharp off-diagonal inequalities for positive Wigner–Smith matrices. A measurement-error corollary converts finite scattering tomography directly into certified degree and delay lower bounds. Reproducible audits include 2,048 random positive matrices and 512 random Blaschke–Potapov products.

Keywords: Wigner–Smith time delay; McMillan degree; passive quantum networks; approximate spectral routing; Grassmannian; rational inner functions; robust interpolation.

1 The result in one picture

A passive network may direct the same input channel toward different output sectors at different frequencies. This behavior underlies multiplexing, reservoir selection and frequency-dependent placement of an operational system–environment boundary. The ideal specification is binary:

$$\text{pass: input subspace lies in sector } A, \qquad \text{stop: it lies in sector } B = A^{\perp}.$$

Real data only certify small leakage. The question is therefore not how many exact transmission zeros a transfer function has, but how far its *output subspace must travel* as frequency changes.

The answer is a geometric action law. Write $\mathcal{X}(\theta)$ for the rank-k output subspace generated by the chosen inputs. A pass-to-stop transition separates the endpoint subspaces by at least $k\alpha$ in the trace-angular Grassmann metric. The positive Wigner–Smith matrix supplies the velocity, but positivity makes motion expensive: at most one half of $\operatorname{tr} Q$ can appear in the off-diagonal block that moves $\mathcal{X}$. Thus

$$\underbrace{2k\alpha}_{\text{required routing motion}} \leq \underbrace{\int_I \operatorname{tr} Q}_{\text{Wigner–Smith memory on the arc}}. \tag{1}$$

The largest eigenvalue of Q controls the same transition without the factor k. Narrow transitions consequently require large proper delays.

The distinction from the exact calibration law in [1] is fundamental. That law counts zeros and gives one unit of degree per exactly lossless direction, even when the calibrated frequencies cluster. Approximate samples alone cannot support such a count. The present result replaces exactness by an ordered routing pattern: approximately pass and approximately stop must alternate. It then recovers the exact coefficient at zero error and remains quantitative at finite error, using only boundary data.

Our contributions are:

1. a nonrational action theorem for every absolutely continuous unitary path with $Q \succeq 0$;
2. additive bounds over arbitrary disjoint frequency arcs;
3. a robust McMillan-degree corollary for rational inner networks;
4. sharp local bounds on trace delay and the largest proper delay;
5. equality constructions in every rank and at every admissible pair of leakage tolerances;
6. a tomography-to-certificate rule that explicitly propagates operator-norm measurement error; and
7. independent numerical stress tests of both proof interfaces.

2 Setup and operational data

2.1 Scattering path and selected inputs

Let $S : \mathbb{T} \to U(N)$ be absolutely continuous. Angles are unwrapped on intervals of $\mathbb{R}$, so we write $S(\theta)$ for $S(\mathrm{e}^{\mathrm{i}\theta})$. Define

$$Q(\theta) = -\mathrm{i}S(\theta)^* S'(\theta). \tag{2}$$

For any unitary path Q is Hermitian. Our passive monotone class assumes

$$Q(\theta) \succeq 0 \quad \text{for almost every } \theta. \tag{3}$$

Every causal rational inner matrix in the disk has this property: a rank-one Blaschke–Potapov factor contributes a positive Poisson kernel, and the product rule preserves positivity by unitary conjugation [2, 3].

Let $J : \mathbb{C}^m \to \mathbb{C}^N$ embed the input ports of interest, and let $V : \mathbb{C}^k \to \mathbb{C}^m$ be an isometry. The selected input projection in the full port space and its output frame are

$$P_0 = JVV^*J^*, \qquad X(\theta) = S(\theta)JV. \tag{4}$$

Thus $X(\theta)^*X(\theta) = I_k$, and $\Pi(\theta) = X(\theta)X(\theta)^* = S(\theta)P_0S(\theta)^*$ is the orthogonal projection onto the routed output subspace $\mathcal{X}(\theta) = \operatorname{ran} X(\theta)$.

Split the outputs into complementary sectors with orthogonal projections R_A, R_B satisfying

$$R_A + R_B = I_N, \qquad R_A R_B = 0. \tag{5}$$

The labels may mean signal/loss, two reservoirs, two spatial ports or two readout classes. No reciprocity, real symmetry or frequency-independent channel basis is imposed on S.

2.2 Approximate routing specifications

At a pass point p and a stop point s, suppose

$$\|R_B X(p)\|_{\mathrm{op}} \le \varepsilon_p, \qquad \|R_A X(s)\|_{\mathrm{op}} \le \varepsilon_s, \qquad 0 \le \varepsilon_p, \varepsilon_s \le 1. \tag{6}$$

These are amplitude leakages. Squared values are worst-case leaked power. Set

$$\alpha(\varepsilon_p, \varepsilon_s) = \left[\frac{\pi}{2} - \arcsin\varepsilon_p - \arcsin\varepsilon_s\right]_+. \tag{7}$$

The bound becomes nontrivial precisely when the two uncertainty cones do not overlap. Equivalently, for $\arcsin\varepsilon_p + \arcsin\varepsilon_s < \pi/2$, define

$$\rho = \sin(\arcsin\varepsilon_p + \arcsin\varepsilon_s), \qquad \alpha = \arccos\rho. \tag{8}$$

3 Three geometric lemmas

The proof separates into endpoint geometry, path geometry and positivity. All three constants will be saturated later.

Lemma 3.1 (Leakage separates the endpoint subspaces)**.** *Under* (5)–(6)*, every canonical angle between $\mathcal{X}(p)$ and $\mathcal{X}(s)$ is at least $\alpha(\varepsilon_p, \varepsilon_s)$.*

Proof. For unit vectors $u, v \in \mathbb{C}^k$, put $a = \|R_B X(p)u\|$ and $b = \|R_A X(s)v\|$. Complementarity and isometry give

$$\|R_A X(p)u\| = \sqrt{1-a^2}, \qquad \|R_B X(s)v\| = \sqrt{1-b^2}.$$

Therefore

$$\begin{aligned} |\langle X(p)u, X(s)v\rangle| &\le \sqrt{1-a^2}\, b + a\sqrt{1-b^2} \\ &= \sin(\arcsin a + \arcsin b) \le \rho, \end{aligned}$$

whenever the angle sum is below $\pi/2$; otherwise the conclusion with $\alpha = 0$ is automatic. Hence $\|X(p)^*X(s)\|_{\mathrm{op}} \le \rho$. The cosines of the canonical angles are the singular values of $X(p)^*X(s)$, so each angle is at least $\arccos\rho = \alpha$. $\square$

For a rank-k subspace path $\mathcal{X}(\theta)$, let

$$L_1(\mathcal{X}; I) = \int_I \|B(\theta)\|_1 \,\mathrm{d}\theta, \qquad L_\infty(\mathcal{X}; I) = \int_I \|B(\theta)\|_{\mathrm{op}} \,\mathrm{d}\theta, \tag{9}$$

where, in the moving frame determined by S,

$$B(\theta) = (I - P_0)Q(\theta)P_0. \tag{10}$$

Only this off-diagonal block changes the output subspace; the diagonal blocks rotate frames inside the subspace and its complement.

Lemma 3.2 (Grassmann distance is no larger than path length)**.** *Let $\beta_1, \dots, \beta_k$ be the canonical angles between the endpoint subspaces of an interval I. Then*

$$\sum_{j=1}^{k} \beta_j \le L_1(\mathcal{X}; I), \qquad \max_j \beta_j \le L_\infty(\mathcal{X}; I). \tag{11}$$

Proof. Differentiate $\Pi = SP_0S^*$ and use $S' = \mathrm{i}SQ$:

$$\Pi' = \mathrm{i}S[Q, P_0]S^*.$$

Relative to $P_0 \oplus (I - P_0)$, the commutator has off-diagonal blocks B and $-B^*$. Thus its nonzero infinitesimal angular velocities are the singular values of B. The symmetric gauge functions $\sum_j \beta_j$ and $\max_j \beta_j$ define the trace-angular and maximum-angular metrics on the Grassmann space [4, 5]. Applying the metric triangle inequality to polygonal refinements of the path and taking the absolutely continuous limit gives (11). □

Lemma 3.3 (Positive generators spend at least twice the motion)**.** *Let $Q \succeq 0$ and $B = (I - P_0)QP_0$. Then*

$$2\,\|B\|_1 \le \operatorname{tr} Q, \qquad 2\,\|B\|_{\mathrm{op}} \le \lambda_{\max}(Q). \tag{12}$$

Both constants are optimal.

Proof. In the decomposition $P_0 \oplus (I - P_0)$ write

$$Q = \begin{bmatrix} A & B^* \\ B & D \end{bmatrix} \succeq 0.$$

Positive block factorization gives $B = D^{1/2}KA^{1/2}$ for a contraction K. Schatten Hölder and arithmetic–geometric mean inequalities yield

$$\|B\|_1 \le \|D^{1/2}\|_2\,\|KA^{1/2}\|_2 \le \sqrt{\operatorname{tr} D\ \operatorname{tr} A} \le \frac{\operatorname{tr} A + \operatorname{tr} D}{2} = \frac{\operatorname{tr} Q}{2}.$$

For the operator norm put $q = \lambda_{\max}(Q)$. Since $\|Q - (q/2)I\|_{\mathrm{op}} \le q/2$ and subtracting a scalar identity does not change the off-diagonal block,

$$\|B\|_{\mathrm{op}} = \|(I - P_0)(Q - (q/2)I)P_0\|_{\mathrm{op}} \le q/2.$$

Equality holds for $Q = (q/2)\left[\begin{smallmatrix} I & -I \\ -I & I \end{smallmatrix}\right]$ on two equal-dimensional sectors. □

4 Sharp robust routing speed limits

Theorem 4.1 (One transition costs Wigner–Smith action)**.** *Let S satisfy* (3)*, and let an interval I have endpoints p, s satisfying* (6)*. With α from* (7)*,*

$$\boxed{\int_I \operatorname{tr} Q(\theta)\,\mathrm{d}\theta \ge 2k\alpha, \qquad \int_I \lambda_{\max}(Q(\theta))\,\mathrm{d}\theta \ge 2\alpha.} \tag{13}$$

If $|I| = \Delta > 0$, then

$$\boxed{\sup_{\theta \in I} \operatorname{tr} Q(\theta) \ge \frac{2k\alpha}{\Delta}, \qquad \sup_{\theta \in I} \lambda_{\max}(Q(\theta)) \ge \frac{2\alpha}{\Delta}.} \tag{14}$$

Proof. By Theorem 3.1, all k canonical endpoint angles are at least α. Hence Theorem 3.2 gives $k\alpha \le L_1$ and $\alpha \le L_\infty$. Integrating Theorem 3.3 proves (13). Dividing the two integral bounds by Δ proves (14). □

The orientation may be reversed: an approximate B endpoint followed by an approximate A endpoint obeys the same result. Pairwise disjoint arcs can therefore be added without double counting.

Theorem 4.2 (Additive routing-action law)**.** *Let $I_1, \ldots, I_L$ be pairwise disjoint arcs. On each arc the selected rank-k subspace changes between complementary sectors with errors $\varepsilon_{p,\ell}, \varepsilon_{s,\ell}$ in either orientation. Put $\alpha_\ell = \alpha(\varepsilon_{p,\ell}, \varepsilon_{s,\ell})$. Then*

$$\boxed{\int_{\cup_\ell I_\ell} \operatorname{tr} Q \, \mathrm{d}\theta \geq 2k \sum_{\ell=1}^{L} \alpha_\ell.} \tag{15}$$

Moreover every arc separately obeys the proper-delay bound $\int_{I_\ell} \lambda_{\max}(Q) \geq 2\alpha_\ell$.

Proof. Apply Theorem 4.1 on each arc and add. Disjointness is the only condition needed for additivity. □

The action law does not use rationality. Rational inner structure converts the available total action into a finite integer. For a rational inner $N \times N$ matrix of McMillan degree n, Blaschke–Potapov factorization gives the exact identity

$$\frac{1}{2\pi} \int_{-\pi}^{\pi} \operatorname{tr} Q(\theta) \, \mathrm{d}\theta = \operatorname{wind}_{\mathbb{T}} \det S = \deg_{\mathrm{McM}} S = n. \tag{16}$$

This is the multichannel Wigner–Smith phase-volume law [6, 7, 8].

Corollary 4.3 (Robust degree certificate)**.** *Under the hypotheses of Theorem 4.2, if S is rational inner of McMillan degree n, then*

$$\boxed{n \geq \frac{k}{\pi} \sum_{\ell=1}^{L} \alpha_\ell.} \tag{17}$$

In particular, suppose M pass points and M stop points occur in strict cyclic alternation, with uniform errors $\varepsilon_p, \varepsilon_s$. The $2M$ intervening arcs are disjoint, so

$$\boxed{n \geq \frac{2Mk}{\pi} \left[\frac{\pi}{2} - \arcsin \varepsilon_p - \arcsin \varepsilon_s \right]_+ .} \tag{18}$$

At exact routing, $n \geq Mk$.

Remark 4.4 (Why ordering replaces exactness). A degree-one interferometer can have arbitrarily many approximate pass samples clustered near one perfect pass point and a single stop elsewhere. Thus sample count without ordering gives no robust degree law. Alternation forces the output subspace to complete a macroscopic excursion between every neighboring pair, which is exactly what (15) counts.

Remark 4.5 (Signed-delay extension). For a general unitary path, Q is Hermitian but need not be positive. The same Grassmann argument still yields

$$\int_I \|Q\|_1 \, \mathrm{d}\theta \geq k\alpha, \qquad \int_I \|Q\|_{\mathrm{op}} \, \mathrm{d}\theta \geq \alpha.$$

Positivity is responsible for the factor two and for replacing absolute delay action by the topological trace in (16).

5 Equality and optimality in every rank

Let

$$H_k = \frac{1}{\sqrt{2}}\begin{bmatrix} I_k & I_k \\ I_k & -I_k \end{bmatrix}, \qquad S_{k,M}(z) = H_k \operatorname{diag}(I_k, z^M I_k) H_k. \tag{19}$$

This is a $2k$-port rational inner matrix. Its McMillan degree is kM and its signal/loss blocks for the first k inputs are

$$G(z) = \frac{1+z^M}{2} I_k, \qquad C(z) = \frac{1-z^M}{2} I_k. \tag{20}$$

On $z = \mathrm{e}^{\mathrm{i}\theta}$ its Wigner–Smith matrix is constant:

$$Q_{k,M} = \frac{M}{2}\begin{bmatrix} I_k & -I_k \\ -I_k & I_k \end{bmatrix}, \qquad \operatorname{tr} Q_{k,M} = kM, \qquad \lambda_{\max}(Q_{k,M}) = M. \tag{21}$$

Proposition 5.1 (Local finite-error equality)**.** *For every admissible $\varepsilon_p, \varepsilon_s$ and every k, M, choose an arc whose interferometric phase $\phi = M\theta$ runs from*

$$\phi_p = 2 \arcsin \varepsilon_p \quad \textit{to} \quad \phi_s = \pi - 2\arcsin \varepsilon_s.$$

Its width is $\Delta = 2\alpha/M$. The endpoint leakages equal the specified errors, and all four inequalities in (13)–(14) *hold with equality.*

Proof. Equation (20) gives $\|C\| = |\sin(\phi/2)|$ and $\|G\| = |\cos(\phi/2)|$. The endpoint subspaces have all canonical angles equal to α. Using (21),

$$\int_I \operatorname{tr} Q = kM\frac{2\alpha}{M} = 2k\alpha, \qquad \int_I \lambda_{\max}(Q) = M\frac{2\alpha}{M} = 2\alpha.$$

The peak equalities follow because both delay quantities are constant. □

Proposition 5.2 (Global exact equality)**.** *The M points $z^M = 1$ are exact pass points and the M points $z^M = -1$ are exact stop points in cyclic alternation. Consequently* (18) *gives $n \geq Mk$, while $\deg_{\mathrm{McM}} S_{k,M} = Mk$. The total action and every one of the $2M$ local trace and proper-delay bounds are also equalities.*

The result is therefore sharp in five independent senses: coefficient in front of M, coefficient in front of k, dependence on the robust angle, local trace delay and local largest proper delay. No unknown architecture constant is hidden in the theorem.

6 From scattering data to a certificate

The theorem can be evaluated from boundary-frequency measurements. It does not require pole fitting, analytic continuation or knowledge of an internal realization.

Suppose only the signal-sector block $G(\theta) = R_A S(\theta) J$ is measured and the full passive model admits a unitary completion. Let $\widehat{G}$ satisfy an operator-norm error bound

$$\left\| (\widehat{G}(\theta) - G(\theta))V \right\|_{\mathrm{op}} \leq \eta_\theta. \tag{22}$$

At a nominal pass point define $g_p = \sigma_{\min}(\widehat{G}(p)V)$, and at a nominal stop point define $g_s = \left\|\widehat{G}(s)V\right\|_{\mathrm{op}}$. Weyl's singular-value perturbation bound and unitarity give certified actual leakages

$$\varepsilon_p^{\mathrm{cert}} = \sqrt{1 - \min\{1, [g_p - \eta_p]_+\}^2}, \qquad \varepsilon_s^{\mathrm{cert}} = \min\{1, g_s + \eta_s\}. \tag{23}$$

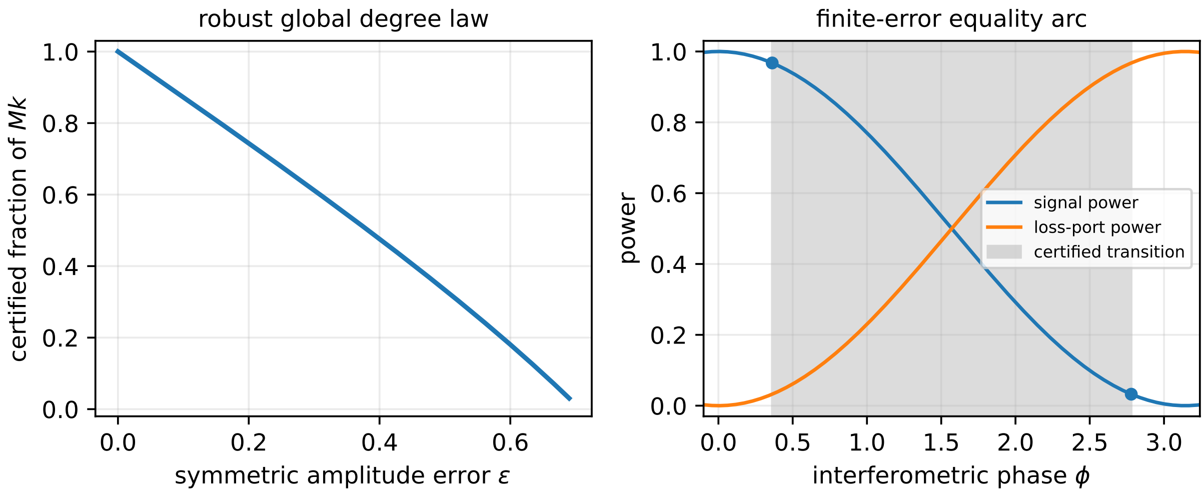

Figure 1: Left: certified fraction of the exact degree law for symmetric amplitude error. Right: an equality arc of the interferometric family; both delay integrals equal their geometric lower bounds on the shaded interval.

Indeed $C^*C = I - G^*G$ on the selected inputs. Substituting the inflated errors into (7) produces a rigorous lower bound. The certificate remains useful whenever

$$\arcsin \varepsilon_p^{\text{cert}} + \arcsin \varepsilon_s^{\text{cert}} < \frac{\pi}{2}.$$

For each adjacent transition the measured angular separation Δ then adds the peak-delay certificate (14). Thus separation is not needed to infer a global degree cost, but it decides how concentrated the unavoidable memory must be. This cleanly separates two experimental questions:

$$\text{how many switches?} \longrightarrow \text{total degree,} \qquad \text{how narrow are they?} \longrightarrow \text{peak delay.}$$

7 Implication for passive quantum reservoirs

In a linear passive quantum network, S routes bosonic input fields among output ports while preserving canonical commutation relations [9, 10]. Choose R_A as the sector coupled to the observed system and R_B as an auxiliary or loss sector. A rank-k bath subspace routed to A at one frequency and to B at another changes which environmental directions reach the system.

For a bath spectral matrix $J_B(\omega)$ with $j_- I \preceq J_B \preceq j_+ I$, the weak-coupling contribution through the signal block is

$$\Gamma_G(\omega) = G(\omega) J_B(\omega) G(\omega)^*. \tag{24}$$

At a pass point with amplitude leakage ε_p, every selected unit input has signal norm at least $\sqrt{1-\varepsilon_p^2}$; at a stop point it has signal norm at most ε_s. Hence the filtered rate scale changes from at least $j_-(1-\varepsilon_p^2)$ to at most $j_+\varepsilon_s^2$ along the selected directions. Repeating this switch M times forces the memory and delay costs above. The rate statement uses the standard weak-coupling interface [11]; the scattering theorem itself is independent of a Markov approximation.

This gives a precise operational reading: moving a quantum noise subspace back and forth across a spectral system–environment boundary cannot be done by a memoryless passive box. The word "memory" refers to internal dynamical degree and Wigner–Smith dwell time, not directly to thermodynamic work or Landauer energy. That distinction follows the resource-boundary outlook of [12] without importing its broader conjectures into the present theorem.

Table 1: Certificate layers. Ratios must not exceed one.

Audit	trials/cases	worst ratio	result
finite-error equality arcs	15	1.000000	equality
exact cyclic families	4	1.000000	equality
positive block, trace norm	2048	0.845291	pass
positive block, operator norm	2048	0.971240	pass
random Potapov paths	512	0.999817	pass

8 Reproducible adversarial audit

The proof is analytic. Numerical experiments are designed to attack its interfaces, not to establish it. The public artifact contains a generator, a frozen JSON ledger and an independent verifier.

The finite-error suite uses $k \in \{1, 2, 4\}$, orders $M \in \{3, 5, 7\}$ and asymmetric as well as symmetric errors. It checks the endpoint overlap, principal angle, arc width and both integrated delays against exact closed forms. The cyclic suite checks degree and total action at orders up to seven and rank four.

The positive-block test draws 2,048 dense complex positive matrices of sizes three through twelve and random projections of every admissible type. It separately attacks

$$\frac{2\|(I-P)QP\|_1}{\operatorname{tr} Q} \le 1, \qquad \frac{2\|(I-P)QP\|_{\mathrm{op}}}{\lambda_{\max}(Q)} \le 1.$$

The path test draws 512 matrix inner products with up to twelve independent rank-one Blaschke–Potapov factors, random subspaces of ranks one through three and independent frequency arcs. It compares the endpoint trace-angular Grassmann distance with half the adaptively integrated Wigner–Smith trace. The most adversarial draw reaches 0.999817 of the bound without crossing it.

The complete replay is:

```
https://github.com/lluiseriksson/finite-sample-spectral-certificates/tree/
research/robust-spectral-routing
```

and the principal commands are

```
python research/routing_speed_limit_certificate.py
python verification/verify_routing_speed_limit.py
python verification/run_routing_speed_limit_release_checks.py
```

9 Relation to existing bounds and priority boundary

Every ingredient used in the proof has a classical life. Wigner and Smith introduced phase and lifetime delay [7, 8]; modern multiport formulations connect the matrix to field-energy overlaps and frequency sensitivity [13]. Canonical angles and unitarily invariant Grassmann metrics are established matrix geometry [4, 5]. McMillan degree and rational inner factorization are standard realization theory [6, 2]. Geometric quantum speed limits provide a useful temporal analogy [14].

Several nearby theories answer different questions. Bode–Fano bounds integrate logarithmic mismatch against load-dependent pole data and their multiport extensions address broadband matching [15, 16]. Boundary and tangential interpolation prescribe complex values or angular derivatives and study solvability or minimal degree [17, 18, 19]. Quantum filter functions quantify noise transfer for specified control protocols [20]. None of these results, in the sources audited here, states the displayed leakage-only chain

$$\begin{aligned}&\text{approximate routing between orthogonal output sectors}\\ &\quad\Longrightarrow \text{Grassmann motion} \Longrightarrow \text{positive Wigner–Smith action}\\ &\quad\Longrightarrow \text{McMillan degree,}\end{aligned}$$

with the sharp constants of Theorems 4.1 and 4.3. This is the specific novelty claim. We do not claim new Grassmann geometry, a new Wigner–Smith definition, a replacement for Bode–Fano theory or a complete solution of robust rational interpolation.

The sequence of preceding papers had progressively narrower comparison loopholes. Noncommuting filters supplied an irreducible construction [21]; passive reservoir filtering converted its amplitude gap into a decoherence-rate gap and exposed a delay price [22]; the exact calibration-memory law replaced a restricted comparator by a universal rational-inner degree bound [1]. The present paper removes the exact-calibration requirement for ordered pass/stop data and extends the action statement beyond rational networks.

10 Scope, failure modes and open problems

Limitation 10.1 (Positive Wigner–Smith class). Arbitrary unitary scattering matrices can have signed proper delays. The sharp factor two and the degree identity apply to the positive class, including causal rational inner matrices in the disk convention used here. For signed paths the absolute-action variant after Theorem 4.3 is the valid statement.

Limitation 10.2 (Fixed input subspace). The same rank-k input subspace is tracked along each certified arc. If the input directions are allowed to change adversarially from sample to sample, the network need not move a common subspace. A useful extension would add a measured correspondence or transport cost between changing input frames.

Limitation 10.3 (Complementary sectors). The clean angle formula uses $R_A + R_B = I$. Additional unmonitored outputs can be included in either sector. If they are left outside both, their leakage must be measured and included in a three-sector angle bound.

Limitation 10.4 (Degree is not hardware energy). McMillan degree, trace delay and proper delay quantify dynamical memory. They do not by themselves determine fabrication volume, temperature, initialization cost or dissipated work. Such conversions require a physical realization model.

The most promising extensions are a measure-valued version for singular inner factors, routing among more than two sectors through a target-subspace graph, and statistical confidence regions for experimentally reconstructed operator norms. A second direction is synthesis: characterize all rational inner matrices attaining the local equalities. The proof shows they must simultaneously saturate the Grassmann geodesic and both positive-block inequalities, strongly constraining their Wigner–Smith generator.

11 Conclusion

Approximate spectral routing has a compulsory memory cost. Each transition of a rank-k input subspace between complementary output sectors covers a robust canonical angle

$$\alpha = \left[\frac{\pi}{2} - \arcsin \varepsilon_p - \arcsin \varepsilon_s\right]_+ ,$$

and positive Wigner–Smith dynamics must spend at least $2k\alpha$ of trace action and 2α of largest-eigenvalue action on that arc. Disjoint transitions add. Rational inner networks have only $2\pi n$ total trace action, so M alternating pass/stop pairs force

$$n \geq \frac{2Mk}{\pi}\alpha.$$

The zero-error law $n \geq Mk$ and both local finite-error delay laws are sharp in every rank. The certificate needs only leakage, ordering and frequency separation measured on the physical boundary. It therefore closes the gap between exact topological calibration counts and finite-error laboratory data while preserving an architecture-independent conclusion.

References

[1] Lluis Eriksson. Lossless calibration is stored memory: A topological McMillan-degree and Wigner–Smith law for passive quantum networks. GitHub release, 2026. Immutable GitHub release.

[2] V. P. Potapov. The multiplicative structure of J-contractive matrix functions. *Trudy Moskovskogo Matematicheskogo Obshchestva*, 4:125–236, 1955. In Russian; English translation in American Mathematical Society Translations, Series 2, Vol. 15.

[3] Daniel Alpay, Palle Jorgensen, and Izchak Lewkowicz. Characterizations of rectangular (para)-unitary rational functions. *Opuscula Mathematica*, 36(6):695–716, 2016.

[4] Li Qiu, Yanxia Zhang, and Chi-Kwong Li. Unitarily invariant metrics on the Grassmann space. *SIAM Journal on Matrix Analysis and Applications*, 27(2):507–531, 2005.

[5] Alan Edelman, Tomás A. Arias, and Steven T. Smith. The geometry of algorithms with orthogonality constraints. *SIAM Journal on Matrix Analysis and Applications*, 20(2):303–353, 1998.

[6] Brockway McMillan. Introduction to formal realizability theory—i. *Bell System Technical Journal*, 31(2):217–279, 1952.

[7] Eugene P. Wigner. Lower limit for the energy derivative of the scattering phase shift. *Physical Review*, 98:145–147, 1955.

[8] Felix T. Smith. Lifetime matrix in collision theory. *Physical Review*, 118:349–356, 1960.

[9] John Gough and Matthew R. James. The series product and its application to quantum feedforward and feedback networks. *IEEE Transactions on Automatic Control*, 54(11):2530–2544, 2009.

[10] John E. Gough and Guofeng Zhang. On realization theory of quantum linear systems. *Automatica*, 59:139–151, 2015.

[11] E. B. Davies. Markovian master equations. *Communications in Mathematical Physics*, 39:91–110, 1974.

[12] Lluis Eriksson. The heisenberg cut as a resource boundary: An operational outlook from coherence maintenance costs. *ai.viXra.org*, 2512.0064v2, 2026.

[13] Utkarsh R. Patel and Eric Michielssen. Wigner–smith time-delay matrix for electromagnetics: Theory and phenomenology. *IEEE Transactions on Antennas and Propagation*, 69(2):902–917, 2021.

[14] J. Anandan and Y. Aharonov. Geometry of quantum evolution. *Physical Review Letters*, 65:1697–1700, 1990.

[15] R. M. Fano. Theoretical limitations on the broadband matching of arbitrary impedances. *Journal of the Franklin Institute*, 249(1–2):57–83, 139–154, 1950.

[16] Wai-Kai Chen. Mathematical theory of broadband matching of multiport networks. *Journal of the Franklin Institute*, 326(5):737–747, 1989.

[17] Joseph A. Ball and Jeongook Kang. Matrix polynomial solutions of tangential Lagrange–Sylvester interpolation conditions of low McMillan degree. *Linear Algebra and its Applications*, 137–138:699–746, 1990.

[18] Joseph A. Ball and Vladimir Bolotnikov. The bitangential matrix Nevanlinna–Pick interpolation problem revisited. *Linear Algebra and its Applications*, 516:122–188, 2017.

[19] Vladimir Bolotnikov. Boundary interpolation by finite Blaschke products. *Complex Analysis and Operator Theory*, 11:1551–1575, 2017.

[20] Pascal Cerfontaine, Tobias Hangleiter, and Hendrik Bluhm. Filter functions for quantum processes under correlated noise. *Physical Review Letters*, 127:170403, 2021.

[21] Lluis Eriksson. Irreducible channel mixing and exponential calibration laws for matrix-polynomial and linear-phase MIMO FIR filters. GitHub release, 2026. Immutable GitHub release.

[22] Lluis Eriksson. Architecture-dependent decoherence suppression in passive quantum networks. GitHub release, 2026. Immutable GitHub release.